

# Analysis of Interaction between Acoustic Waves and CH<sub>4</sub>/Air Laminar Partially Premixed Flames by means of OH-PLIF

T. Pagliaroli<sup>\*</sup>,

R. Bruschi, E. Giacomazzi, M. Marrocco, C. Stringola, E. Giuliotti

*ENEA, TER- SIST/IMP, S.P. 081, Via Anguillarese 301, 00123*

*S.M. Galeria, Rome, Italy*

G.P. Romano

*University "La Sapienza", Via Eudossiana 18, 00184*

*Rome, Italy*

## Abstract

The aim of this paper is to characterize the dynamics of reaction zones in CH<sub>4</sub>-AIR laminar combustion focusing on their interaction with external forced acoustic waves. PLIF (Planar Laser Induced Fluorescence) methodology is used to sample OH field, that is known to be related to the flame front. Identification and tracking of laminar flame boundaries,  $\Psi(x,y,t)$ , are performed by means of an in-house software tool, Flame Front Detector (FFD). The algorithms used in FFD to filter OH\* field and track flame boundaries are described and discussed. By analysing  $\Psi(x,y,t)$  it is possible to show the effect of acoustic waves on laminar flame boundaries: acoustic perturbations can wrinkle, stretch and tilt flame surface. This work shows the existence of a correlation between the tilt angle and the emitted acoustic pressure signal.

*Key words: laminar flames dynamics, flame front boundaries, planar laser induced fluorescence, acoustics, combustion.*

---

<sup>\*</sup> Corresponding Author. Tel.: +39.063048.3370

E-mail address: [tiziano.pagliaroli@alice.it](mailto:tiziano.pagliaroli@alice.it)

## Nomenclature

$Re$  : Reynolds number

$\Phi$  : equivalence ratio

$p'_n$  : standardized acoustic pressure

$f^*$  : resonance frequency

$q'$  : heat-release rate

$p'$  : fluctuating value of pressure oscillations

$V$  : flow domain

$\vec{u}$  : particle velocity

$e$  : acoustic energy

$\dot{e}_{ac}$  : source term in acoustic energy equation

$\overline{F}$  : PLIF image

$\overline{F}_f$  : filtered PLIF image

$\overline{K}$  : kernel of Gaussian filter

$\overline{F}$  : average of  $\overline{F}_f$

$\overline{F}_{bin}$  : binary PLIF image

$\Psi(x, y)$  : flame front line

$\lambda(x, y)$  : linear fitting of  $\Psi(x, y)$

$\phi$  : flame front tilt angle

$\overline{\phi}$  : mean of  $\phi$  on 50 samples

$\overline{\phi}_n$  : standardized  $\overline{\phi}$

## Introduction

In the last years, the interest for interaction between acoustics and premixed flames did grow a lot. Sometimes this interaction generates a thermo-acoustic instability phenomenon, called *humming*, that may damage combustors proportionally to the power of the system. In fact in conditions of incipient extinction the sound pressure level (SPL) can reach high critical values and, at the same time, burners submitted to instabilities usually have a higher efficiency and consequent higher  $\text{NO}_x$  emission rate.

Thermo-acoustic instability establishes when the acoustics of the system generates a feedback mechanism between fluctuations of pressure and heat release. The acoustic signal generated in the combustion chamber modulates fuel feeding and changes local fuel-air ratio, thus making heat release unsteady.

In the context of gas turbines, burning at lean operating conditions is attractive from the point of view of reduced  $\text{NO}_x$  formation; on the other hand, in propulsion devices, such as ramjet engines, burning under near stoichiometric conditions is desirable since this leads to enhanced heat release and therefore high performance. Interestingly enough, both of these conditions lead to potentially unstable behavior.

Currently little is known about the mechanisms by which the flame responds to the acoustic feedback and understanding these mechanisms is an area of active investigation.

A suitable device to investigate these phenomena is Planar Laser Induced Fluorescence (PLIF) methodology. Recently however, the application of high repetition rate PLIF imaging has been applied for quantitative study and to provide data for comparison with numerical simulations<sup>[1]</sup>. PLIF images show concentration of fluorescent chemical species in the flame; if chemical species relevant to ignition are chosen as tracers, PLIF provide information about flame front topology and development of flame for complete characterization of the process. In this work an efficient and simple adaptive threshold algorithm for flame edge detection is proposed, together with a composite convolution filter to remove PLIF high frequency noise.

### 1. Coupling between Acoustic Field and Heat Release Dynamics

The combustion process can be subdivided into sub-dynamics: acoustics, convective phenomena, molecular transport processes, chemical kinetics, flame kinematics, heat transfer and feedline dynamics of the reactants. These sub-dynamics can be coupled with each other in many different ways, as illustrated in Figure 1.1

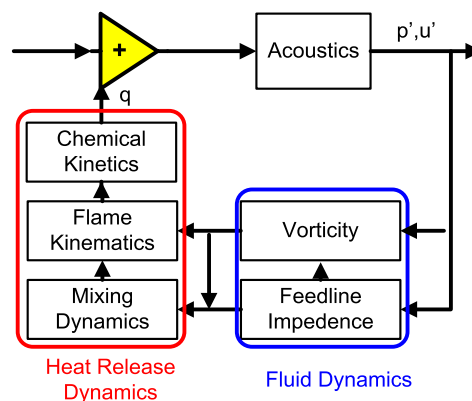


**Figure 1.1:** schematic diagram of the acoustics, fluid dynamics and heat release dynamics and of their interactions.

The schematic diagram in Figure 1.1 illustrates the dependence between acoustic field and other sub-dynamics. The general equation for acoustic energy,  $e$ , that describes these dependence, can be derived as

$$\frac{\partial e}{\partial t} + \nabla \cdot (E) = \dot{e} \quad (1)$$

$$e = \frac{\overline{\rho u'^2}}{2} + \frac{p'^2}{2\rho c^2},$$

Where  $E$  is the generalized acoustic energy flux and  $\dot{e}$  is the source term including unsteadiness in heat and mass addition, entropy fluctuations, and vorticity fluctuations. Since the system dominant dynamics are those of heat release and acoustic waves, neglecting the viscous terms, the Eqn. (1) for acoustic energy is simplified and represented as<sup>[2]</sup>

$$\frac{\partial e}{\partial t} + \nabla \cdot (p' \vec{u}') = \frac{\gamma - 1}{\gamma p} p' q' \quad (2)$$

$$\dot{e}_{ac} = \frac{\gamma - 1}{\gamma p} p' q'$$

Where  $\dot{e}_{ac}$  is a source term in Eqn. (2) and it refers to the energy coupling between heat release rate and acoustic field, unsteadily induced by the flame itself. If this pressure wave is in phase with heat release, a closed loop is established and self-amplification of the pressure field can be observed. Formally, this criterion may take the following form (Lord Rayleigh postulate<sup>[3]</sup>):

$$G(x) = \iiint_V q'(x,t) p'(x,t) dV$$

The sign of the above integral may change with the phase of the oscillation; if  $p'$  and  $q'$  are in phase  $G(x) > 0$ , thus combustor instability is realized.

## 2. Experimental set-up

In the flame front, chemical reactions determine the local change of temperature and the production of radicals, such as CH and OH. The interplay between the two phenomena is very useful in that radicals are particularly suitable to mark regions of high temperatures. It is, indeed, well known that OH radicals are good indicators of the flame front position<sup>[4]</sup>. To that end, an experiment aimed at the detection of OH fluorescence has been carried out according to the above-mentioned PLIF technique.

In our set-up, a Nd:YAG laser is used to create a light sheet that induces fluorescence of OH\* radicals at a wavelength of about 283 nm. The intensity of fluorescence emitted by the radicals OH\* is a function of their local concentration and is measured by means of an intensified CCD camera (ICCD). In this manner, the technique allows the analysis of a planar region within the flame.

Inside the combustion chamber a generator of acoustic waves is used to produce external forcing. It consists in a 200 W tweeter (CIARE PT 382). A microphone (in our case Larson Davis 2541) acquires the signal generated by the tweeter.

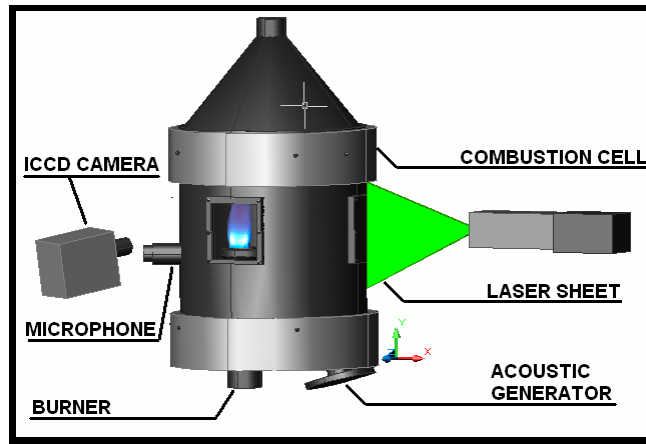


Figure 2.1: experimental set-up for PLIF.

The burner, fed with a  $\text{CH}_4/\text{Air}$  mixture, is equipped with a conical bluff-body to anchor the flame. The bluff-body produces a toroidal recirculation zone which mixes hot products and reactants, preheats them, and increases their residence time, thus anchoring the flame. Inside the burner there is a pre-mixer but the combustion is not perfectly premixed and the flame front is thick and boundaries are evident.

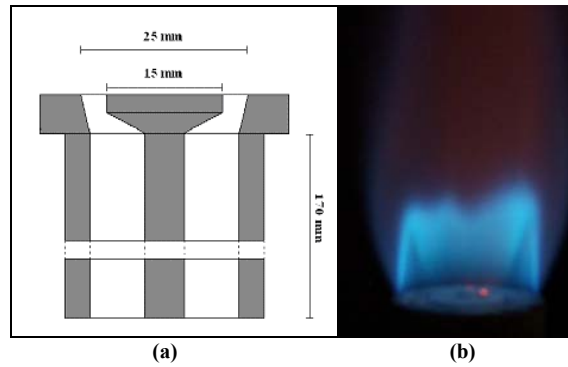


Figure 2.2: (a) burner section; (b) laminar flame picture.

### 3. PLIF-Image Processing Stage

#### 3.1 Filter for Raw PLIF Image

PLIF images ( $\overline{F}$  being the associated 2D-array,  $m \times n$  dimensional) are acquired with ICCD camera. They are affected by noise introduced by the camera sensor; this makes boundary tracking very difficult, therefore  $\overline{F}$  is filtered by means of median and Gaussian convolution filters applied in series.

The *median* filter, that is based on *statistic ordering*, is indicated for highly inhomogeneous images to eliminate so called “outliers”, i.e., samples that can be associated to noise (organized in small clusters in the images).

Then a *Gaussian* filter is applied to the already median filtered  $\overline{F}$ ; gaussian filtering is mathematically expressed as a convolution integral, that in discrete form becomes<sup>[5]</sup>

$$F_{ij} = \sum_{k=-1}^1 \sum_{w=-1}^1 F_{i+k, j+w} \cdot K_{2+k, 2+w}$$

where  $\overline{\overline{K}}$  is the Gaussian kernel<sup>†</sup>. It is a smoothing filter and it dampens high-frequency noise.

In Figure 3.1 (a) an acquired PLIF image is shown; in Figure 3.1 (b) the associated filtered PLIF image,  $\overline{\overline{F_f}}$ , is shown. Now it is possible to process the image to mark the flame front boundaries.

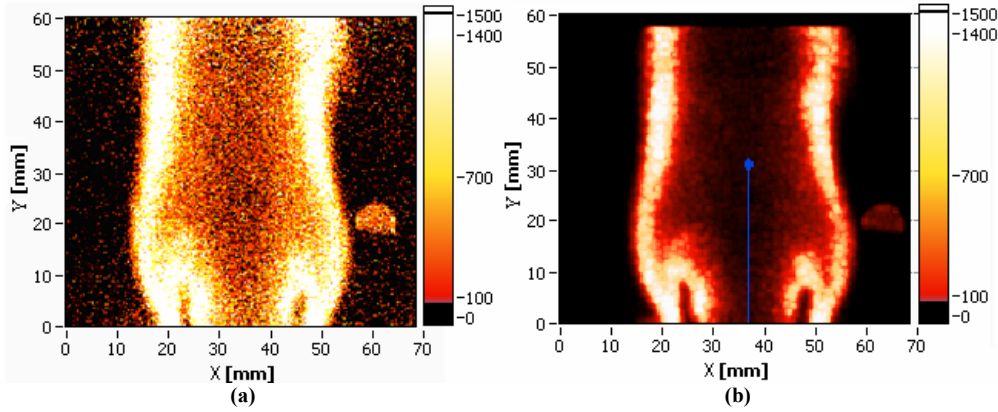


**Figure 3.1:** (a) raw signal  $\overline{\overline{F}}$ ; (b) filtered signal  $\overline{\overline{F_f}}$ .

### 3.2 Flame Front Tracking by means of OH\* Field

To mark the flame front boundaries,  $\Psi(x,y)$ , the ensemble average  $\overline{\overline{F}}$  of  $\overline{\overline{F}}$  is calculated as:

$$\overline{\overline{F}} = \frac{1}{m \cdot n} \sum_{i=1}^m \sum_{j=1}^n F_{ij}$$

This  $\overline{\overline{F}}$  is used as auto-threshold to transform  $\overline{\overline{F_f}}$  into a binary form,  $\overline{\overline{F_{bin}}}$ , by means of the following operator:

$$\overline{\overline{F_{bin}}} = \begin{cases} 1, & F_f(x, y) \geq \overline{\overline{F}} & (\text{inside the flame front}) \\ 0, & F_f(x, y) < \overline{\overline{F}} & (\text{outside the flame front}) \end{cases}$$

---

<sup>†</sup>  $\overline{\overline{K}} = \frac{1}{209} \begin{bmatrix} 16 & 26 & 16 \\ 26 & 41 & 26 \\ 16 & 26 & 16 \end{bmatrix}$

Computer experiments indicate that the set of points belonging to the flame front boundaries  $\Psi(x,y)$  is efficiently identified via:

$$\Psi(x,y) = \left\{ P(x,y) \in \overline{\overline{F_{bin}}} \left| \sum_{i=-1}^1 \sum_{j=-1}^1 \overline{\overline{F_{bin}}}(x+i, y+j) \leq 8 \wedge \overline{\overline{F_{bin}}}(x,y) = 1 \right. \right\}$$

If  $\overline{\overline{F_{bin}}}(x,y) = 1$ ,  $P(x,y)$  is inside the reaction zone (where  $\text{OH}^*$  concentration is high) and if  $\overline{\overline{F_{bin}}}(x+i, y+j) \leq 8$ , there is at least one zero (where  $\text{OH}^*$  concentration is low) inside a rectangular around of  $P(x,y)$ , therefore  $P(x,y)$  belongs to boundaries.

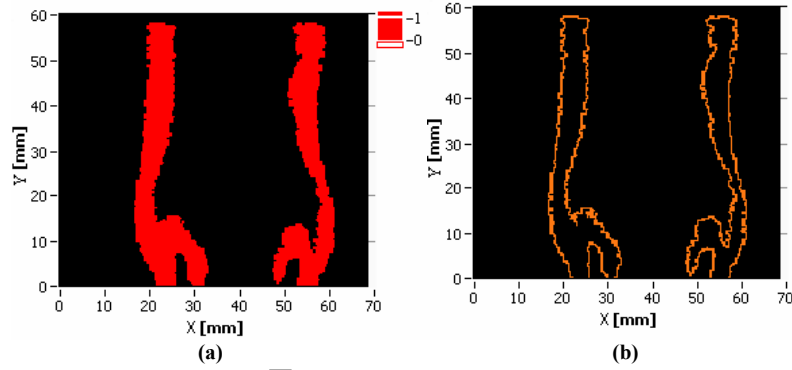


**Figure 3.2:** : (a) binary form of  $\overline{\overline{F_f}}$  called  $\overline{\overline{F_{bin}}}$ ; (b) flame front boundaries obtained by processing.

#### 4. Analysis of Interaction between a $\text{CH}_4$ -Air Laminar Premixed Flame and Acoustic Waves

The sinusoidal emitted signal by the acoustic generator, controlled by means of a function generator whose tension is 200 mV, is sampled by means of a microphone in two configurations:

1. the sole acoustic generator is considered emitting in ambient air;
2. the flame is confined and the acoustic signal is emitted putting the generator inside the combustion chamber.

In Figure 4.1 it is shown that in configuration 1 acoustic pressure is nearly constant in the range of frequencies considered and that in configuration 2 the signal is maximum at  $f^*=2260$  Hz (resonance frequency of process).

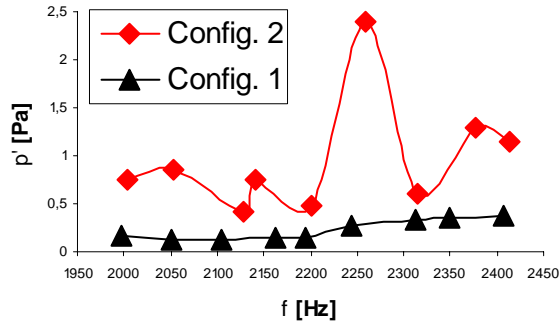


**Figure 4.1:** amplitude of acoustic wave emitted in two different configurations: 1 in ambient air, 2 inside the combustion chamber.

The effect of the signal emitted on the flame front topology of a laminar  $\text{CH}_4/\text{Air}$  premixed flame ( $\text{Re}=2000$ ,  $\Phi=0.6$  and  $f=2260$  Hz) is shown in Figure 4.2 (b).



**Figure 4.2:** (a) flame; (b) flame excited by external acoustics.

PLIF and sound pressure are sampled for the laminar flame examined. By means of the strategy previously described, FFD (Flame Front Detector), it is possible to calculate  $\lambda(x,y)$ , the linear fitting of  $\Psi(x,y)$ :

$$\lambda(x,y) = ax + by$$

$\lambda(x,y)$  is approximately the axis of symmetry of the flame. The coefficients  $a$  and  $b$ , obtained by linear fitting of  $\Psi(x,y)$ , are used to calculate the tilt angle  $\phi$ :

$$\phi = \frac{\pi}{2} - \text{tg}^{-1}\left(-\frac{a}{b}\right)$$

$\phi$  is nearly nil when acoustic waves are not present (Figure 4.3).

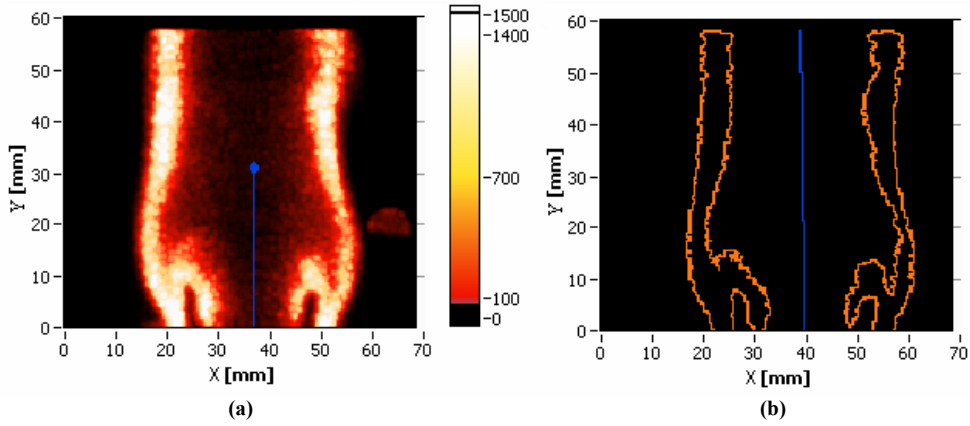


**Figure 4.3:** (a) PLIF; (b)  $\Psi(x, y)$  and  $\lambda(x, y)$  obtained with FFD processing.

In Figure 4.4 the mean  $\bar{\phi}_n$  on 50 samples of  $\phi$  and acoustic pressure  $p'_n$  are represented. The subscript n indicates that all the values are standardized with respect to peak values.

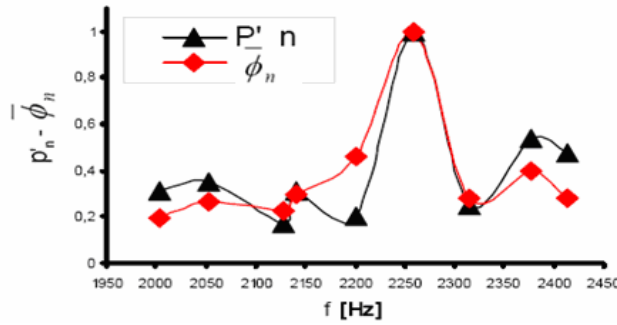


**Figure 4.4:** acoustic pressure and tilt angle of the flame in the acoustic forced case.

Figure 4.4 shows that the tilt angle  $\bar{\phi}_n$  is maximum at the acoustic resonance frequency  $f^*$ ; the associated value of cross-correlation coefficient,  $R_{xy}$ , between  $\bar{\phi}_n$  and  $p'_n$ , is very high ( $R_{xy} = 0.9999$ ).

Thus, the relationship between  $\bar{\phi}_n$  and  $p'_n$  is linear for  $f \in [2 \text{ kHz}; 2.4 \text{ kHz}]$  (the range of frequencies examined), and it is possible to write  $\bar{\phi} = mp' + c$  with  $m, c$  constants.

In Figure 4.5, PLIF images of the flame and the associated flame boundaries are shown in forced and non forced acoustic conditions.

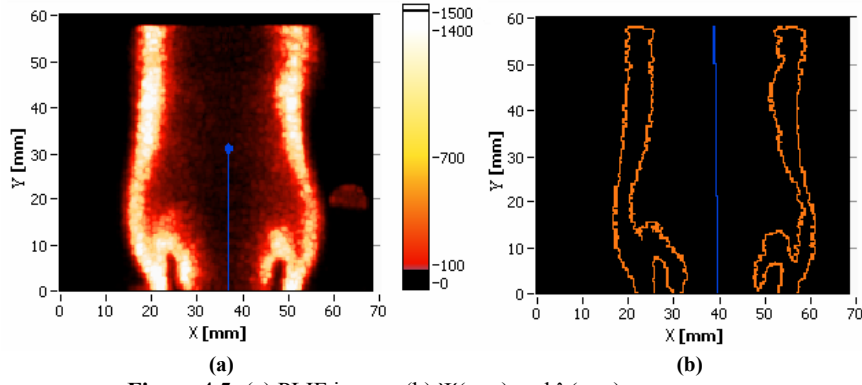


**Figure 4.5:** (a) PLIF image; (b)  $\Psi(x, y)$  and  $\lambda(x, y)$ .

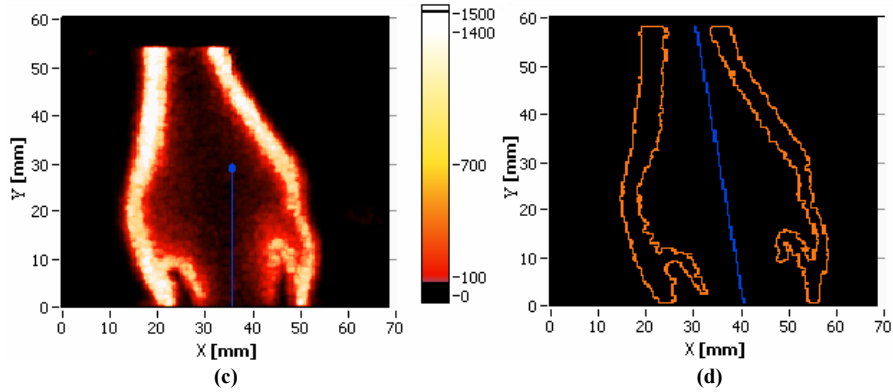


**Figure 4.6:** (c) PLIF image forced with  $f^* = 2260$  Hz; (d)  $\Psi(x, y)$  and  $\lambda(x, y)$ .

**Table:** values obtained from FFD processing.

Re	$\Phi$	$P'$ [Pa]	$\phi$ [deg]	$\sigma(\phi)$ [deg]	f [Hz]
2000	0.6	0	1.47	4.5	0
2000	0.6	2.40	15.95	3.9	2260

In synthesis a global effect of external acoustics on flame front has been observed and this effect is linear with the signal amplitude  $p'$ .

## 5. Discussion and Conclusions

The FFD Software, implemented on Labview 7.1, can be used to reveal local effects on flame front: dynamics, stretching, wrinkling, tilting and combustion instabilities. The algorithms implement in FFD are efficient to extract flame front boundaries from large experimental data sets; in fact, they work with laminar as well as turbulent flames.

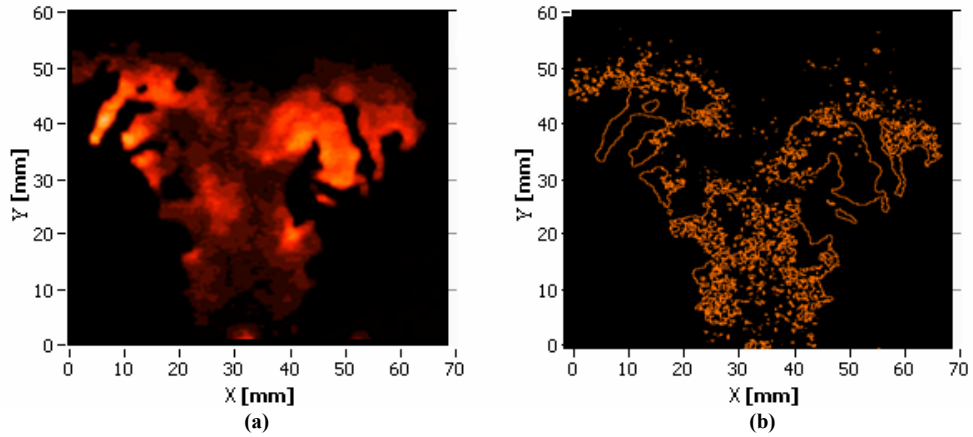


**Figure 5.1:** (a) PLIF image of turbulent flame  $Re=9600$ ; (b)  $\Psi(x, y)$  of turbulent flame.

The capability to track the flame boundaries in time is a unique way to study turbulent flame dynamics. In this work it was shown that the flame tilting produced by acoustic wave can be extracted. As future work also wrinkling of the flame, related to local reaction rates, will be obtained; the software will be integrated with a subroutine Fluid-dynamics Structure Detector (FSD) to obtain, by means of Particle Image Velocimetry (PIV) technique, the flow field to characterize the interactions between turbulent premixed flame, acoustic waves and flow field.

## 6. Acknowledgements

Thanks to L. Sinisi, E. Stefanutti and M. Nobili for their crucial help and useful discussions. Finally thanks also to F. Manfredi, V. Casasanta, for their help in laboratory experiences and to S. Giammartini for his support.

## References

- [ 1 ]Anuradha M., Annaswamy A., Ghoniem F., Active Control of Combustion Instability: “Theory and Practice”, IEEE Control Systems ISSN 10066-033x, Vol. **22**, pp. 6:37-54, 2002.
- [ 2 ]Poinsot T., Veynante D., *Theoretical and Numerical Combustion*, Edwards, Philadelphia, 2001.
- [ 3 ]Zinn B.T and Neumeier Y., “Application of Rayleigh’s Criterion in Active Control of Combustion Instabilities in Gas Turbines”, ISABE 99-7180, 1999
- [ 4 ]Abu-Gharbich R., Hamarneh G., Gustavsson T., Kaminiski F.C., “Flame front tracking by laser induced fluorescence spectroscopy and advanced image analysis”, Optics Express, Vol. **8**, pp. 5:278-287, 2001.
- [ 5 ]Pratt W.K., *Digital image processing*, John Wiley & Sons, New York, 1991.
- [ 6 ]C.F. Kaminski, J. Hult, and M. Ald’en, “High repetition rate planar laser induced fluorescence of OH in a turbulent non-premixed flame”, Appl. Phys. B 2000, Vol. **68**, pp. 757-760, 2000.